# Title: Conditions for coexistence of β-lactamase mutants

**Running title: Ecological feedbacks limit spread of a β-lactamase mutant**

Philip Ruelens[1*], Eline de Ridder[1], J. Arjan G.M. de Visser[1, #], Meike Wortel[2,#]
[1] Laboratory of Genetics, Wageningen University & Research, Wageningen, The Netherlands
[2] Molecular Biology and Microbial Food Safety, Swammerdam Institute for Life Sciences, University of Amsterdam, Amsterdam, The Netherlands

#Address correspondence to: arjan.devisser@wur.nl, m.t.wortel@uva.nl

*Present address: Philip Ruelens, Laboratory of Socioecology and Social Evolution, KU Leuven, Leuven, Belgium

## Abstract

Antibiotic resistance in bacterial infections is a growing global health concern, with β-lactamases playing a pivotal role. Understanding the origin and spread of β-lactamases can provide insights for developing novel drugs and therapies. However, complexity arises by the fact that they can affect their own selective advantage through antibiotic degradation, which also shields nearby susceptible bacteria. To address this eco-evolutionary feedback, we investigated the interplay between feedbacks and the spread of bacterial strains expressing different β-lactamase enzymes conferring varying levels of resistance to the cephalosporin cefotaxime (CTX). Specifically, we conducted head-to-head competitions between two related clinically relevant β-lactamase mutants, TEM-19 and TEM-52, and varied CTX concentration and cell density to explore the impact of these factors on competitive fitness and coexistence. Results revealed that at certain antibiotic treatment regimes, culture density, which modulated the eco-evolutionary feedback strength, determined whether resistance alleles could invade the population and replace or coexist with susceptible alleles. Furthermore, using a population dynamic model based solely on measured parameters, we investigated the underlying mechanisms of the observed dynamics. By validating our model with experimental data, we show that it can largely predict the equilibrium frequencies based on dose-dependent growth rates and antibiotic degradation activities of the individual strains. Our study emphasizes the importance of considering ecological feedbacks in the evolution of antibiotic resistance, even at the level of individual proteins, and highlights the potential of a predictive model applicable to clinically relevant conditions.

## Introduction

Antibiotic resistance is a major global health threat that poses a significant challenge to modern medicine (1). The emergence and spread of resistant bacterial strains have rendered many antibiotics ineffective, leading to longer hospital stays, and an increase in morbidity and mortality (2). β-lactamases, a family of enzymes that hydrolyze β-lactam antibiotics, are among the most common and clinically relevant antibiotic resistance determinants (3). Given their importance, the evolutionary dynamics of β-lactamase resistance have been extensively studied (4–6). A complicating factor, which has been ignored in most studies, is the potential influence of eco-evolutionary feedback on the invasion of new β-lactamase variants due to antibiotic removal by the β-lactamases themselves, which may significantly impact their competitive fitness and hence spread (7–12). A more quantitative understanding of the effect of eco-evolutionary feedback on the spread of bacteria expressing β-lactamases is therefore required for a comprehensive understanding of the dynamics of resistance evolution.

In population dynamics, invasion fitness is a common metric to assess whether a mutant can successfully invade and establish itself within a population (13). Although mutations often become fixed in the whole population, negative frequency dependent selection, i.e., the benefit of a mutation decreases when it becomes more frequent, can hinder this process. In the context of antibiotic resistance , this can occur when resistance mutations decrease the environmental antibiotic concentrations, thereby benefitting less resistant mutants — a phenomenon known as cross-protection (7, 14–16). Cross-protection has been observed in high-density bacterial populations (7, 11, 14, 17, 18), including for clonal populations, where the effectiveness of an antimicrobial agent may decrease with increasing bacterial density, referred to as 'inoculum effect' (17). Cross-protection may obstruct resistance evolution, and, if it leads to coexistence, could lead to recovery of the susceptible type when antibiotic pressure diminishes. For cross-protection to lead to coexistence, it is necessary that resistance confers a cost – the susceptible strain needs to grow faster without antibiotics to recover from its inhibition. This cost is evident when antibiotic resistance determinants are located on a plasmid, but can also occur from single nucleotide polymorphisms affecting the activity of an enzyme (19). The extent to which competing bacteria expressing different antibiotic-degrading enzymes may influence each other's evolution, and thereby the protein's fitness landscape, through eco-evolutionary feedbacks remains unclear. In scenarios where these competing alleles are involved, the fitness costs might be significantly lower compared to those associated with plasmid-acquired resistance, which could limit the potential for cross-protection to lead to coexistence.

In order to successfully spread, bacteria expressing more active antibiotic-degrading β-lactamase enzymes must outcompete the susceptible bacteria from which they derive via mutation. Essentially, both strains engage in a competition for limited resources, while particularly the more resistant strain removes antibiotic from the environment through enzymatic degradation (Figure 1). When the initial concentration of the antibiotic is above the minimum inhibitory concentration (MIC) of the relatively susceptible strain, the relatively resistant strain may rescue the more susceptible strain if the antibiotic concentration is reduced below the MIC of the susceptible strain before it is completely eliminated by the antibiotic. If so, the susceptible strain can resume growth and potentially increase in relative frequency when the resistant strain exhibits a lower fitness in the absence of antibiotic (17). Population density plays a crucial role in these competitive interactions, as high-density bacterial populations can degrade antibiotics more rapidly, enhancing the probability of susceptible bacteria to survive until the antibiotic concentration decreases below inhibitory concentrations. At low densities, in contrast, resistant bacteria can grow longer without competition from susceptible bacteria, allowing their relative frequency to increase more and/or the susceptible population to be killed entirely. The critical density allowing survival of susceptible bacteria clearly also depends on the initial antibiotic concentration. Interestingly, when the resistant strain has lower fitness than the susceptible strain in the absence of antibiotic, conditions allowing the rescue of the susceptible bacteria by the resistant strain may lead to the stable coexistence of both strains during the serial transfers.

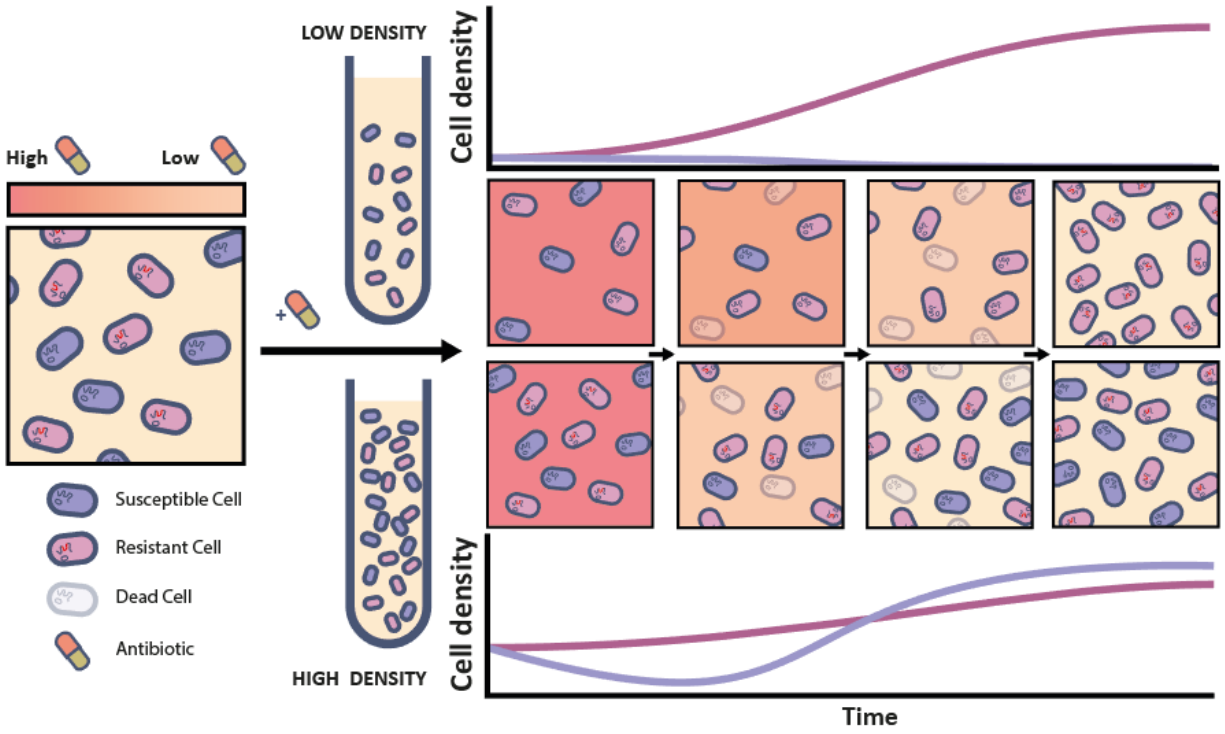


**Figure 1. Schematic depiction of competition between resistant bacteria expressing an antibiotic-degrading enzyme (pink) and susceptible bacteria (purple) in the presence of antibiotic (background shades of red).** The enzyme inactivates the antibiotic in the environment, creating conditions for susceptible bacteria to grow in the presence of resistant bacteria. The relative fitness of both strains is density-dependent, as high-density bacterial populations can degrade antibiotics more rapidly, providing susceptible bacteria with the ability to survive under otherwise lethal antibiotic concentrations.

In this study, we aim to investigate the extent to which ecological feedback caused by antibiotic degradation can influence the evolution of resistance conferred by mutations in the naturally occurring narrow-spectrum β-lactamase TEM-1. TEM-1 efficiently inactivates penicillins and first generation cephalosporins, but just a few mutations are required to confer resistance to an extended spectrum of β-lactams with serious clinical consequences (20–22). To understand how resource competition and antibiotic breakdown affect the fitness of a resistant relative to a susceptible strain, we competed two *E. coli* strains expressing different extended spectrum TEM alleles (hereafter called β-lactamase mutants), in the presence of varying concentrations of the third-generation cephalosporin cefotaxime (CTX): TEM-19 (called "susceptible") and TEM-52 (called "resistant"), with relatively low and high activity against CTX, respectively. Moreover, we varied cell density through nutrient availability to vary the rate of antibiotic breakdown, and therefore the level of eco-evolutionary feedback. To quantitatively understand

the experimental outcomes, we developed a population dynamic model that interrogates how physiological parameters and ecological conditions influence the evolution of resistance. Our results demonstrate a crucial role for ecological feedbacks mediated by antibiotic degradation and resource competition in shaping the relative fitness of the competing strains and determining whether susceptible bacteria may stably coexist alongside resistant ones or not.

## Results

### *Population density and antibiotic concentration mediate coexistence between β-lactamase mutants*

To explore the extent by which antibiotic concentration and cell density affects the fitness of bacteria expressing different variants of an antibiotic-degrading enzyme, we conducted a serial passage competition experiment between two isogenic strains of *Escherichia coli* carrying different TEM β-lactamase alleles: TEM-19 and TEM-52. These alleles are noteworthy as they signify clinically relevant variations in the mutational landscape of TEM-1 β-lactamase, leading to cefotaxime resistance, while differing in only two mutations (TEM-19 with the G238S mutation, and TEM-52 with mutations E104K, M182T, and G238S). Nevertheless, TEM-52 exhibits an MIC for the third-generation cephalosporin cefotaxime (CTX) that is more than three orders of magnitude higher than that of TEM-52 ($MIC_{TEM-19}$ = 1.0 µg/ml, $MIC_{TEM-52}$ = 4,096 µg/ml; Supplementary Data 1). Thus, while both strains are able to degrade CTX, they do so at highly different rates (24), henceforth TEM-19 will be referred to as the susceptible strain and TEM-52 as the resistant strain. To distinguish between these two strains, the susceptible and resistant strain were chromosomally labelled with yellow (YFP) and blue fluorescent protein (BFP), respectively. Importantly, the expression of these fluorescent proteins did not differentially affect fitness (Supplementary Figure 1).

Susceptible and resistant strain were mixed together at ratios of 1:9, 1:1, and 9:1 in eight biological replicates each. The final yield of the culture, or population carrying capacity, was varied by supplementing glycerol as the sole carbon source to a final concentration of 0.2%, 0.4%, 0.9%, or 2%. Furthermore, we investigated the impact of three different initial antibiotic concentrations: 50, 25, or 12.5 µg/ml CTX. We performed a total of five serial transfers and determined the fraction of resistant and susceptible bacteria after each growth cycle by counting the number of YFP and BFP cells (cells/ml) using a flow cytometer. Our results show that the susceptible strain, expressing TEM-19, managed to survive at antibiotic concentrations significantly higher than its MIC in the presence of the resistant TEM-52 strain (Figure 2A). For conditions with initial antibiotic concentrations of 12.5 and 25 µg/ml, we observed a gradual decline in the fraction of resistant cells over time, stabilizing at approximately 0.21, seemingly

independent of the initial glycerol concentration. However, we did observe an intriguing exception to this trend in competitions initiated with a 1:9 ratio of resistant to susceptible bacteria at low glycerol concentrations. Here, the fraction of resistant cells surged rapidly during the initial growth cycle, leading to an overshoot of this equilibrium and apparent extinction of the susceptible strain. At an antibiotic concentration of 50 µg/ml, we observed that the average final fraction of resistant cells decreased from 0.92 to 0.43 with increasing glycerol concentrations, showing the density-dependent nature of protection of susceptible by resistant cells.

That the fractions stabilize over the transfers, increasing to this value from a lower initial fraction and decreasing form a higher initial fraction, suggests that there is a fraction at which there is a dynamic equilibrium. In this equilibrium, the fractions still fluctuate over each transfer, but in exactly the same manner, leading to the same fraction at the beginning and the end of each transfer. We inferred the stable equilibrium frequency of the resistant bacteria for each replicate growth series. Equilibrium values were derived by interpolating the relationship between initial and final fractions (Figure 2B, Supplementary Information S1; see Yurtsev et al. 2013). We then employed generalized linear models to explore the influence of glycerol and CTX, along with their interaction, on the equilibrium frequency of resistant cells. Our findings indicate that incorporating the interaction of glycerol x CTX significantly improved the model fit (including interaction: AICc = -71.78; excluding interaction: AICc = -69.95; Interaction effect: $\chi_1^2 = 3.97$, p= 0.046). The antibiotic concentration also significantly affected the equilibrium frequency independently of glycerol (main effect antibiotic: $\chi_1^2$ = 36.19, p<0.0001), while glycerol alone did not have a significant effect (main effect glycerol: $\chi_1^2$ = 0.016, p<0.90). Our results revealed that the effect of glycerol on the equilibrium frequency was modulated by the antibiotic concentration. In particular, we found that glycerol had little impact at low CTX levels, but significantly determined equilibrium frequencies at high antibiotic concentrations (Figure 2C).

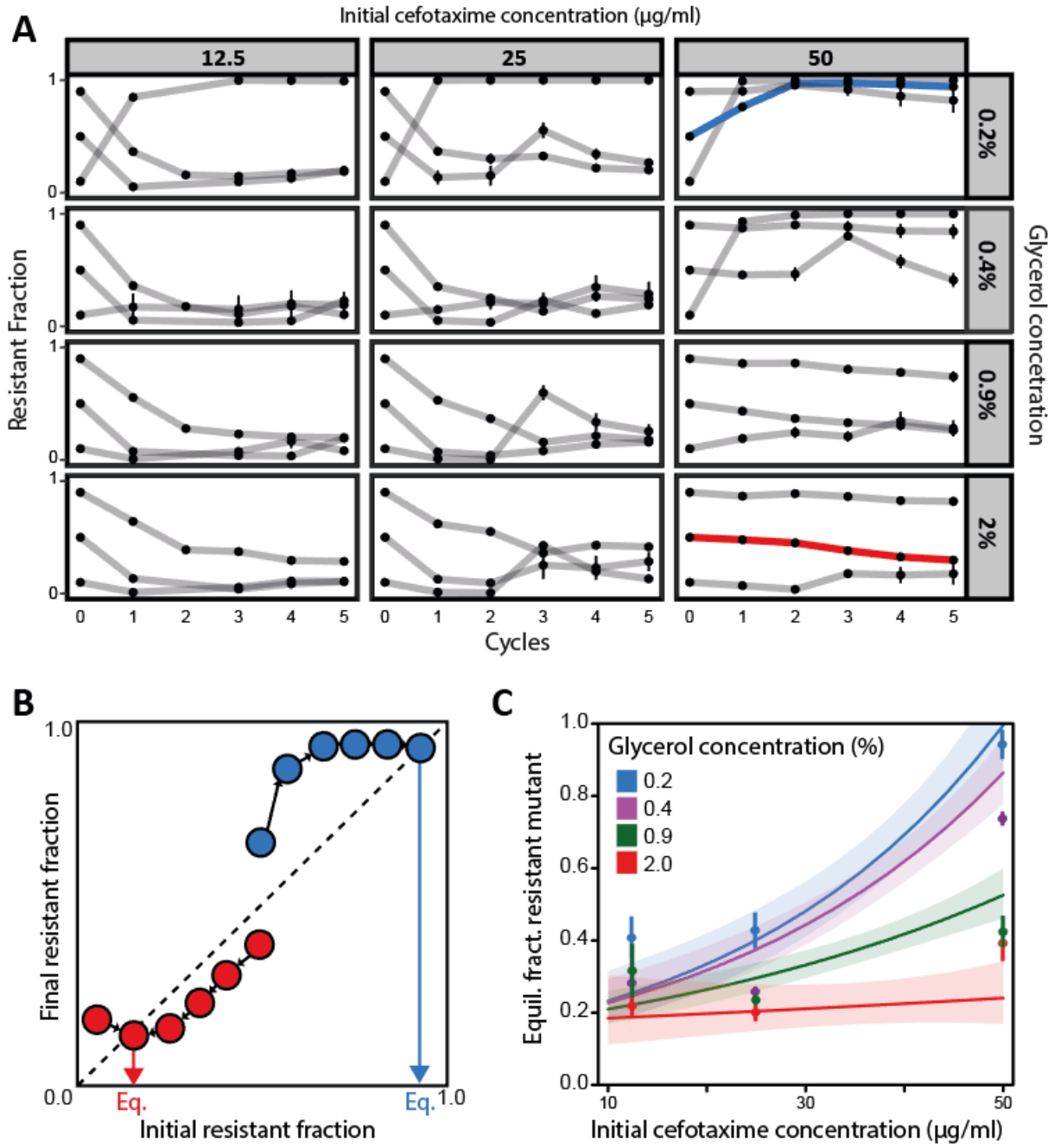


**Figure 2. Conditions for coexistence of antibiotic-resistant and susceptible strain. (A)** Line plots showing the fraction of the resistant strain expressing TEM-52 β-lactamase in mixed cultures together with a relatively susceptible strain expressing TEM-19 β-lactamase across five serial transfers under different starting ratios, cell densities (varied by varying glycerol concentrations) and CTX concentrations. The error bars represent the standard error of the mean from eight biological replicates. Note that the error bars are not always visible due to the small standard error at that point. **(B)** Procedure to predict the equilibrium frequency of the resistant strain

from experimental data by plotting the resistant frequency every iteration during serial transfer. The equilibrium is reached when the lines connecting subsequent frequencies cross the diagonal. The crossing of the diagonal will be lower for high densities (red) than for low densities (blue). **(C)** Plot showing the joint impact of glycerol and CTX on the equilibrium fraction of resistant bacteria. The shaded areas represent the smoothed 95% confidence interval around the model estimated means (depicted by the thicker lines). Raw data means and standard errors are also depicted as dots and vertical bars.

### *Physiological model predicts competitive dynamics and coexistence*

We then constructed a model that could predict the competitive dynamics and coexistence of two strains as function of the antibiotic concentration and cell density based on basic physiological parameters. We expanded a previously used model with death in stationary phase and antibiotic degradation by the more susceptible strain, two properties that we observed in our system (7). The model parameters include the maximal growth rate, the death rate and antibiotic clearance rate of each strain. The maximal growth rates (0.185±0.00326 $h^{-1}$ for the resistant and 0.190±0.00219 $h^{-1}$ for the susceptible strain) showed indeed a small but significant cost of the resistance mutations, which is a necessary condition for coexistence. The death rate of the resistant strain (1.54±0.186 $h^{-1}$) was higher than expected. Although we found faster degradation of the resistant strain as expected, this seems mostly caused by increased affinity (24), and we even report a higher estimated maximal degradation rate of the susceptible strain ($6.69*10^{-4} \pm 3.36*10^{-4}$ µg $cell^{-1}$ $h^{-1}$ versus $3.10 * 10^{-4} \pm 9.15*10^{-5}$ µg $cell^{-1}$ $h^{-1}$ of the resistant strain), although that is never reached because of the low affinity. We estimated these parameters in experiments (Supplementary Data 1) and used their values to parameterize our model and predict the change in the relative frequencies of the strains at each passage (see Fig. 2A).

When accounting for only these basic properties, our model predicts that a higher initial antibiotic concentration favors the more resistant strain, while a higher cell density favors the more susceptible strain (Figure 3A). Because the dilution rate is fixed in these simulations, increasing the cell density increases both the initial and final population size. The first affects the dynamics, because a higher initial population size causes a faster degradation of the antibiotic, and the second because a higher final population size allows for a longer growth period once the antibiotic is sufficiently degraded. Both these effects favor the more susceptible strain, which explains that the equilibrium frequency of the resistant strain is both antibiotic and density-dependent (Figure 3A). Moreover, the range of CTX and glycerol concentrations that allow for coexistence largely agree with the previously described general linearized model derived from the experimental measurements (Figure 3A and B).

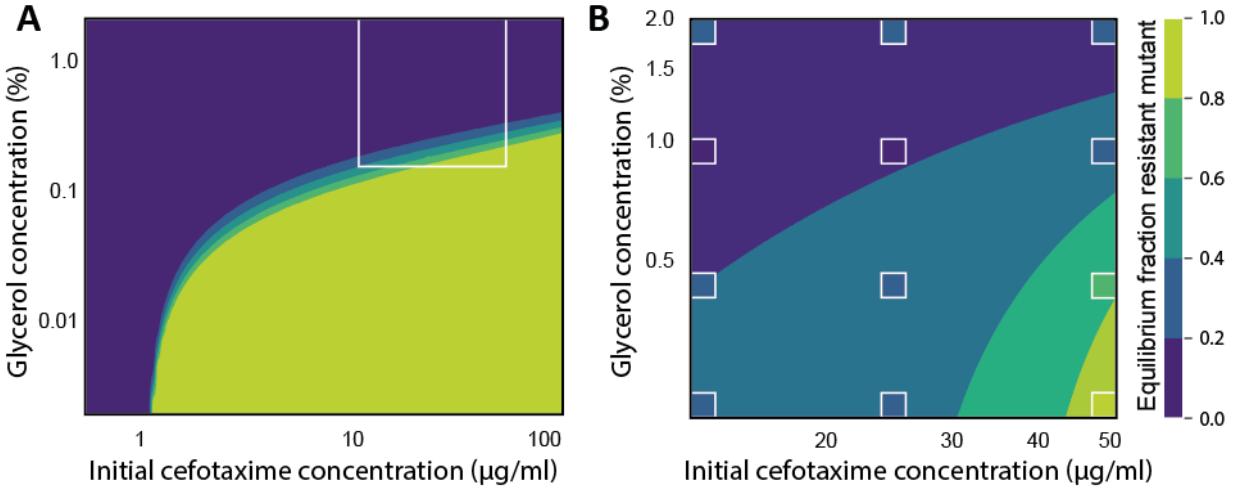


**Figure 3: Model predictions of the equilibrium resistant frequency. (A)** Contour plot showcasing model-projected equilibrium frequencies of the resistant strain under a wider range of parameter values than the experimental data, using physiological parameter measurements from both strains, across a variety of conditions. The region within the white box corresponds to the experimentally examined range depicted in the contour plot of (B). **(B)** Contour plot, interpolating the statistical model represented in Figure 2C, demonstrating how the equilibrium frequencies of the resistant strain change concerning concentrations of glycerol and cefotaxime. White boxes indicate the experimental raw data means.

### *Effect of cell density on coexistence in continuous culture*

Whereas serial-passage experiments include cycles of resource supply and population size, natural conditions are often more similar to a continuous regime. We modeled this with a continuous culture model with antibiotics added in pulses to mirror the clinical daily dosage administration of antibiotics (similar results are obtained for continuous administration of antibiotics, see Supplementary section S.3). Under this framework, the average population size is regulated by adjusting nutrient concentrations in the inflow, while the actual population sizes fluctuate with the antibiotic pulses (Figure 4A). Consequently, culture density remains relatively constant, eliminating the initial population size variable. However, the impact of cell density on the competitive dynamics and coexistence of antibiotic-resistant strains remains highly relevant and qualitatively similar to our previous results. For a large range of antibiotic administration regimes, the outcome of the competition between the susceptible and resistant strain depends on the population size (Figure 4B).

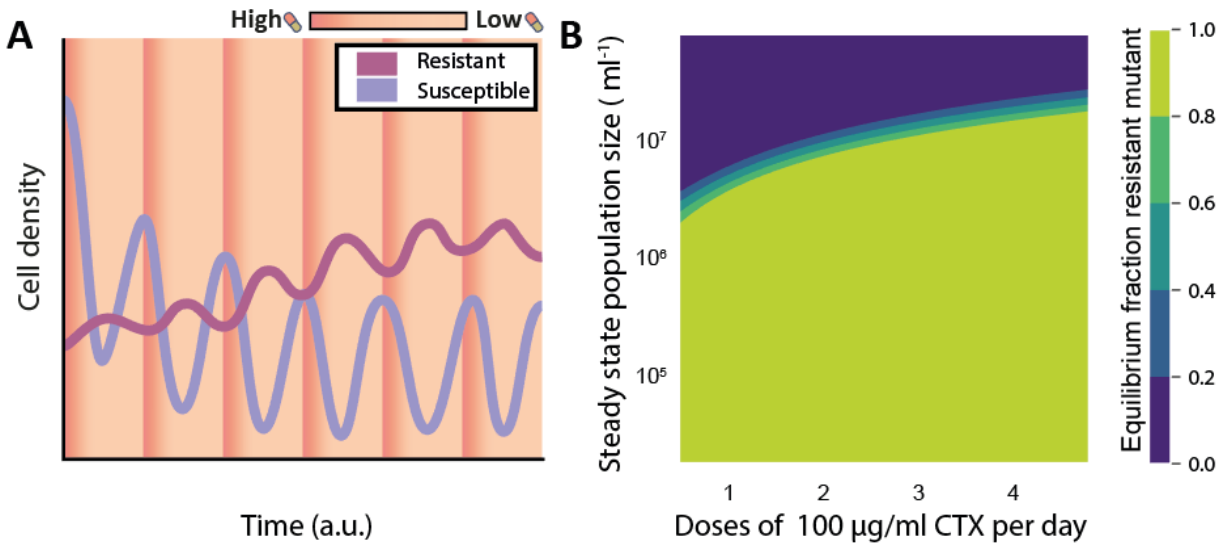


**Figure 4. Modelling competition and coexistence under continuous nutrient input. (A)** The model parameterized with the physiological parameters (Supplementary Data 1) and validated on the serial transfer experiments (Figure 3) is simulated in a continuous culture with antibiotic pulses (shown as shades of orange). After a pulse, the susceptible population decreases due to death and washout, which increases the nutrient availability for the resistant population, which therefore increases. The resistant cells degrade the antibiotic to a level at which the susceptible population recovers, which reduces the nutrient availability and thereby the resistant population. After an initial dynamic period, the fluctuations become regular and the ratio between the strains at the start of each pulse reaches an equilibrium. **(B)** Antibiotic pulses to a mixed population of bacteria expressing different TEM β-lactamase variants with constant nutrient supply shows a density dependent effect on the equilibrium of the two TEM variants. Cell densities and nutrients are modeled as a continuous culture and CTX is modeled as regular pulses that lead to a concentration of 100 µg/ml in the culture. The growth rates of the two strains are modelled with a logistic function that depends on the CTX concentration and was experimentally obtained and a nutrient dependent term with an arbitrary but equal affinity.

## Discussion

The complex interplay between antibiotics and resistance mechanisms involving antibiotic degradation vividly illustrates the concept of ecological feedback. Understanding the evolutionary role of antibiotic degradation and other feedback mechanisms is essential for a comprehensive understanding of the emergence and spread of antibiotic resistance. To shed light on this topic, we explored the potential for eco-evolutionary feedback via antibiotic degradation to modulate relative fitness and facilitate the coexistence of near-isogenic strains

with distinct levels of antibiotic resistance. Specifically, we focused on strains carrying different alleles of the antibiotic-inactivating β-lactamase enzyme TEM-1, that differ by just two mutations, resulting in differences in their degradation efficiency of CTX. However, despite these minor genetic changes, these mutations may introduce variable costs (19), as evidenced by differences in growth rates in the absence of antibiotics, which results in a dynamic fitness profile of both strains that is not only dependent on the antibiotic concentration, but also the culture density and the relative frequency of the strains. This dynamic fitness profile ultimately dictates whether one strain dominates and becomes fixed within the population, or whether a state of coexistence is achieved. It is important to emphasize that in our study, when varying the culture cell density by adding different levels of glycerol, we kept the number of generations constant, allowing us to decouple the effect of the number of competitive generations and the culture density on competition outcome. This deviates from the approach taken by Yurtsev et al. (2013), who demonstrated that the initial cell density achieved by varying dilution factors can affect the equilibrium fraction. Moreover, previous studies of coexistence via exposure protection (7, 25, 26) typically involved coexistence between a susceptible population and a population with resistance conferred through the introduction of an antibiotic resistance gene. This approach can introduce genetic differences other than the resistance mechanism between the two populations, resulting in more pronounced fitness differences. Our results demonstrate that eco-evolutionary feedback from antibiotic degradation resulting from single mutations can qualitatively affect the outcome of competition, with resistant mutants compromising their own selective advantage and frustrating the trajectory of evolution.

Antibiotic concentrations experienced by a bacterial population are dynamic and determined by a multitude of factors, including physical environmental conditions such as temperature and pH, as well as the metabolic activities of the bacteria themselves (17). Here, we have studied the effect on the competitive success of bacteria expressing different β-lactamases, which can reduce environmental antibiotic concentrations (17, 25, 27). Earlier modeling work examining a small set of TEM-1 β-lactamase mutants found that the evolution of CTX resistance via mutations enhancing CTX degradation is dependent on the administered antibiotic concentrations (28). In another study, the coexistence of susceptible and plasmid-mediated ampicillin resistant populations has been shown to lead to the evolution of the susceptible strain towards greater antibiotic tolerance without significant increases in resistance, unlike monocultures where resistance would increase (8). Our study demonstrates that exposure protection also occurs among subtly different alleles of the TEM-1 gene, indicating the importance of eco-evolutionary feedback interactions for the evolution of β-lactamase alleles

with enhanced activity against the β-lactam used for selection. Our findings demonstrate that predictions of evolutionary trajectories of antibiotic resistance relying on traditional resistance measurements, such as MIC (6), do not accurately capture the complex dynamics governing resistance evolution. Instead, determining relative fitness through competition experiments becomes imperative to account for unavoidable eco-evolutionary feedback processes.

Our experiments revealed that in some cases, there was a marked increase in the resistant fraction, at times even leading to the extinction of the susceptible population, especially when the resistant fraction is initially low. This phenomenon can be attributed to the low number of resistant cells, which keeps the antibiotic concentration at elevated levels for an extended period. As a result, the susceptible population experiences a rapid and substantial decline that cannot be compensated for by subsequent growth. This trend, which we observed in our experiments, has also been reported in a previous study (7), and is also replicated in our model, underscoring its validity.

We modified a population dynamic model with very basic physiological parameters of the two strains. Our results show that we can largely understand the quantitative outcomes based on the properties of the individual strains, which we have validated with experimental data. Our model's ability to predict coexistence without the need for parameter estimation during model fitting (in contrast to previous similar approaches (e.g. (7)), indicates that our model successfully captured the most relevant factors for predicting the effect of ecological feedbacks in various scenarios. Importantly, our model allowed us to make predictions beyond the laboratory setting and translate our results to a more clinically relevant continuous culture with pulsed antibiotic administration, demonstrating that the observed patterns hold true in more realistic scenarios.

While our model successfully captures the feedback effect of antibiotic degradation on the selective benefit of a more active β-lactamase allele, it has limitations compared to natural populations and conditions. One of the limitations is that our study is limited to mutations enhancing the activity of the β-lactamase and does not consider compensatory mutations that can reduce the costs of resistance, which may reduce the potential for cross-protection to frustrate the evolution of antibiotic resistance. This also means we do not consider other, more private, mechanisms of resistance, such as target modification or decreased intake or increased efflux of antibiotics, which will come with different potential for eco-evolutionary feedback (29, 30). Expanding our model to include spatially-structured conditions, such as those found in biofilms, is also important. These environments are more representative of natural conditions

and may significantly influence the dynamics we've observed (11, 26, 31). Nevertheless, our study offers valuable insights into the intricate relationship between the dynamics of selective conditions and β-lactamase evolution, underscoring the need to consider the complexity of the system when developing novel approaches to combat antibiotic resistance. By acknowledging these factors, we can develop more effective strategies to prevent the emergence and spread of antibiotic resistance, ultimately leading to improved health outcomes.

## Methods

### *Strains, plasmids and medium*

The *Escherichia coli* strain used throughout this study was BW27783 (CGSC#12119), which lacks arabinose metabolizing genes and expresses *araE* from an arabinose independent promoter allowing stringent control of the arabinose-inducible promoter, pBAD (32). Plasmid pBAD332T was used as the expression vector to express TEM-1 and its alleles, TEM-19 (G238S) and TEM-52 (E104K-M182T-G238S)(33). To differentiate between the two different alleles during the coexistence experiment, BW27783 was labelled with a yellow (YFP) or blue (BFP) fluorescent marker by inserting cat-J23101-SYFP2 or cat-J23101-mTagBFP2 into chromosomal *galK* using the Quick and Easy *E. coli* Gene Deletion Kit (Gene Bridges, Heidelberg, Germany).

TEM alleles were amplified from previously described plasmid constructs (34), ligated into pBAD322T using T4 DNA ligase (New England Biolabs), and then electroporated into *E. coli* DH5α. After verifying successful cloning via sequencing, isolated plasmid was transformed into BW27783, BW27783-YFP and BW27783-BFP. All experiments were performed in M9 minimal media (supplemented with 0.2% Casamino acids, 1µg/mL thiamine, and 10 µg/ml tetracycline to prevent plasmid loss). Glycerol was added to the medium as carbon source to a final concentration of 0.4% unless otherwise stated. L-arabinose (0.000625% or otherwise stated) was used to express the TEM-alleles.

### *Growth rate, death rate and minimum inhibitory concentration*

To determine the growth rate of BW27783 expressing TEM alleles TEM-19 or TEM-52, 200 µL M9 medium supplemented with cefotaxime and L-arabinose in a 96-well microtiter plate was inoculated at a 1:200 dilution from overnight culture in M9. The samples were subsequently covered with 50 µL mineral oil to prevent evaporation and condensation of the lid. The 96-well plate was incubated for 24h at 37 °C in a Victor3 microtiter plate reader (PerkinElmer, Waltham, MA, USA), and absorbance was measured every three minutes. The plate was shaken (double orbital) for 30 seconds before each measurement. Growth rates represent the maximum linear slope of the natural logarithm of absorbance versus time in a 2 h window and were determined using a custom python script.

The death rate of BW27783 expressing TEM-19 was estimated by performing a time-kill experiment. Bacteria from an overnight culture grown in M9 medium supplemented with L-arabinose were exposed to 25 µg/ml cefotaxime. After 0, 2 and 6 hours of incubation at 37°C, the number of colony forming units per ml were determined by plating on LB agar plates and counting the number of colonies formed after overnight incubation. The death rate was

calculated as the slope of the regression line describing the logarithm of the bacterial density as a function of time.

We determined the minimum inhibitory concentration of cefotaxime of both TEM mutants using the liquid broth microdilution method (35). From overnight culture in M9 medium, approximately 200,000 cells were transferred to 200µl of M9 medium supplemented with cefotaxime and L-arabinose. Plates were incubated for 24 h at 37 °C with agitation. The minimum inhibitory concentration was visually assessed and defined as the lowest cefotaxime concentration where no growth could be observed.

Growth rate and minimum inhibitory concertation were determined for BW27783 carrying pBAD322T-TEM-19 and BW27783 with pBAD322T-TEM-52. Death rate was only determined of BW27783 expressing TEM-19.

### *Estimating the in vivo cefotaxime degradation rate*

To qualitatively asses the *in vivo* degradation rate of both β-lactamase alleles, we developed a bioassay based on the agar diffusion assay (36). In this assay, we estimated the remaining cefotaxime concentration in medium inoculated with BW27783 carrying either pBAD322T-G238S or pBAD322T-E104K-M182T-G238S after defined time intervals. Each strain was initially cultured overnight in 5ml M9 medium supplemented with 10 µg/ml tetracycline and 0.000625% arabinose at 37°C with continuous shaking at 250 rpm. After 16 hours of incubation, the OD600 of these samples were measured in a spectrophotometer and the cells were pelleted and resuspended in 5ml M9 medium with cefotaxime but without glycerol. The initial concentration cefotaxime for the TEM-19 mutant was 32 µg/ml and for TEM-52 4096 µg/ml. These samples were incubated at 37°C and, after 15-, 30- and 45 minutes, cell-free supernatants (CFS) were prepared and placed on ice. The CFS was prepared by pelleting down 1.4 ml culture and filter sterilizing the supernatants using a 0.22 µm filter. From the CFS of each mutant, an eight times two-fold dilutions series was made in M9 medium. At each time point, the number of colony-forming units (CFUs) was determined by collecting 1 ml culture of each mutant after 0, 15, 30 and 45 min by plating a 10,000-fold dilution on LB-agar plates and counting the number of colonies following incubation overnight.

In order to assess the remaining concentration of cefotaxime at different time points, a control dilution series with known cefotaxime concentrations was also prepared. LB-agar plates were streaked with 100 µl of overnight culture of the cefotaxime susceptible WT BW27783. Four holes were punctured in the agar arranged in equidistant positions with a pipette tip (P100). Each hole was filled with 100 µl from the control dilution series (in triplicate) or 100 µl from the

CFS-dilutions series of each mutant (in triplicate) and incubated at 37°C for one day. As the susceptible WT strain cannot grow at high CTX concentrations, a zone of inhibition (ZOI) was visible on the plates of which the diameter was measured using a ruler. A calibration curve was prepared by plotting the known CTX concentrations of the control dilution series and its measured ZOI. The resulting equation was subsequently used to predict the amount of remaining CTX based on the ZOI. For each time point, the predicted concentration was divided by the average CFUs between the current time point and the previous one. The result of this was plotted against time, resulting in a linear relationship. The slope of this line represents the estimated degradation rate (ug $cell^{-1}$ $h^{-1}$)

### *Coexistence experiment*

To investigate the impact of population density and antibiotics on two strains carrying either TEM-19 or TEM-52, which were chromosomally labeled with yellow or blue fluorescent protein, we conducted a serial passage competition experiment. The induced overnight cultures were counted using a flow cytometer and mixed to three starting ratios (1:9, 1:1, and 9:1) in eight biological replicates. Then, these mixed cultures were transferred to 96-well plates containing M9 medium supplemented with glycerol (0.2, 0.43, 0.93, or 2%) and cefotaxime (50, 25, or 12.5 µg/ml) to a final volume of 200 µl. The starting population size of each condition was 200 times less than the maximum cell number in the respective conditions. To ensure that the culture was fully saturated, we incubated it for 48 hours at 37°C. After 48 hours of incubation with shaking, each culture was diluted 20-fold and transferred to a new 96-well plate with freshly prepared M9 medium supplemented with glycerol and cefotaxime at the appropriate concentrations, and this serial transfer was repeated five times. Following each growth cycle, each culture was diluted 100-fold in a new plate containing cold M9-medium before being counted using a MACSQuant10 flow cytometer(Miltenyi biotec, Bergisch Gladbach, Germany). We conducted flow cytometry analysis with a moderate flow rate using SSC 1.4 as a trigger, and we counted a total of 20,000 events for each sample. For obtaining the equilibrium ratio from the experimental data, see Supplementary information section S.1.

Data analysis was conducted using R statistical software (v3.6.1) accessed through RStudio (Build 576). To assess the relationship between the equilibrium fraction and antibiotic concentration and density, a generalized linear model was applied using the 'glm' function (base R package). Model selection was based on the second-order Akaike information criterion using 'AICc' implemented in the 'MuMIn' package.

### *Model description*

We follow the modeling approach from (7), extending their Model 7 with two additions. We observe death in the lag phase and our susceptible strain also degrades the antibiotic. Therefore, we have included a death term in the lag phase and degradation by the susceptible strain. Including either of these features makes it impossible to directly calculate the equilibrium fractions, therefore we have resorted to numerical methods to obtain the equilibrium fractions (see supplementary Jupyter notebook).

Our model contains the following set of equations:

For $t < \tau_{lag}$:

$$\frac{dN_R}{dt} = 0$$

$$\frac{dN_s}{dt} = \begin{cases} 0, & A < MIC \\ -\gamma_D N_s, & A \geq MIC \end{cases}$$

$$\frac{dA}{dt} = -V_{max,R} N_R \frac{A}{A + K_{M,R}} - V_{max,S} N_S \frac{A}{A + K_{M,S}}$$

For $t > \tau_{lag}$:

$$\frac{dN_R}{dt} = \gamma_R N_R$$

$$\frac{dN_s}{dt} = \begin{cases} \gamma_S N_s, & A < MIC \\ -\gamma_D N_s, & A \geq MIC \end{cases}$$

$$\frac{dA}{dt} = -V_{max,R} N_R \frac{A}{A + K_{M,R}} - V_{max,S} N_S \frac{A}{A + K_{M,S}}$$

With $N_R$ the population size of the more resistant strain TEM-52, $N_s$ of the more susceptible strain TEM-19 and $A$ the antibiotic concentration. For the parameters see Supplementary Table S.1. See the supplementary information for the sensitivity analysis and the continuous culture model.

## Acknowledgments

This study was supported by grants from the Human Frontiers in Science Program (RGP0010/2015) to JAGMdV, the Netherlands organization for scientific research (OCENW.XS.058) to JAGMdV and an EMBO fellowship (ALTF 273-2017) to PR.

## Declaration of interests

The authors declare no competing interests.

## Appendices

**Supplementary Figure 1:** Relative competitive fitness of BW27783 carrying BFP to BW27783 carrying YFP. The statistical insignificance was assessed using the one-sample Wilcoxon non-parametric test.

**Supplementary Information:** Supporting information including Supplementary Section S1 (Equilibrium Ratio from Experimental Data), S2 (Serial Transfer Model), and S3 (Continuous Culture Model), Supplementary Tables S1, S2, and S3, as well as Supplementary Figures S1 through S4.

**Supplementary Data 1:** Source data underlying Figure 2 and Figure 3A.

**Supplementary Code:** https://github.com/WortelLab/tem1coex/

## References


1. Murray CJ, Ikuta KS, Sharara F, Swetschinski L, Robles Aguilar G, Gray A, Han C, Bisignano C, Rao P, Wool E, Johnson SC, Browne AJ, Chipeta MG, Fell F, Hackett S, Haines-Woodhouse G, Kashef Hamadani BH, Kumaran EAP, McManigal B, Agarwal R, Akech S, Albertson S, Amuasi J, Andrews J, Aravkin A, Ashley E, Bailey F, Baker S, Basnyat B, Bekker A, Bender R, Bethou A, Bielicki J, Boonkasidecha S, Bukosia J, Carvalheiro C, Castañeda-Orjuela C, Chansamouth V, Chaurasia S, Chiurchiù S, Chowdhury F, Cook AJ, Cooper B, Cressey TR, Criollo-Mora E, Cunningham M, Darboe S, Day NPJ, De Luca M, Dokova K, Dramowski A, Dunachie SJ, Eckmanns T, Eibach D, Emami A, Feasey N, Fisher-Pearson N, Forrest K, Garrett D, Gastmeier P, Giref AZ, Greer RC, Gupta V, Haller S, Haselbeck A, Hay SI, Holm M, Hopkins S, Iregbu KC, Jacobs J, Jarovsky D, Javanmardi F, Khorana M, Kissoon N, Kobeissi E, Kostyanev T, Krapp F, Krumkamp R, Kumar A, Kyu HH, Lim C, Limmathurotsakul D, Loftus MJ, Lunn M, Ma J, Mturi N, Munera-Huertas T, Musicha P, Mussi-Pinhata MM, Nakamura T, Nanavati R, Nangia S, Newton P, Ngoun C, Novotney A, Nwakanma D, Obiero CW, Olivas-Martinez A, Olliaro P, Ooko E, Ortiz-Brizuela E, Peleg AY, Perrone C, Plakkal N, Ponce-de-Leon A, Raad M, Ramdin T, Riddell A, Roberts T, Robotham JV, Roca A, Rudd KE, Russell N, Schnall J, Scott JAG, Shivamallappa M, Sifuentes-Osornio J, Steenkeste N, Stewardson AJ, Stoeva T, Tasak N, Thaiprakong A, Thwaites G, Turner C, Turner P, van Doorn HR, Velaphi S, Vongpradith A, Vu H, Walsh T, Waner S, Wangrangsimakul T, Wozniak T, Zheng P, Sartorius B, Lopez AD, Stergachis A, Moore C, Dolecek C, Naghavi M. 2022. Global burden of bacterial antimicrobial resistance in 2019: a systematic analysis. The Lancet 399:629–655.
2. Cosgrove SE. 2006. The Relationship between Antimicrobial Resistance and Patient Outcomes: Mortality, Length of Hospital Stay, and Health Care Costs. Clinical Infectious Diseases 42:S82–S89.

3. Bush K, Jacoby GA. 2010. Updated Functional Classification of β-Lactamases. Antimicrobial Agents and Chemotherapy 54:969–976.
4. Barlow M, Hall BG. 2002. Predicting evolutionary potential: in vitro evolution accurately reproduces natural evolution of the TEM β-lactamase. Genetics.
5. Schenk MF, Zwart MP, Hwang S, Ruelens P, Severing E, Krug J, de Visser JAGM. 2022. Population size mediates the contribution of high-rate and large-benefit mutations to parallel evolution. Nature Ecology & Evolution.
6. Weinreich DM. 2006. Darwinian Evolution Can Follow Only Very Few Mutational Paths to Fitter Proteins. Science.
7. Yurtsev EA, Chao HX, Datta MS, Artemova T, Gore J. 2013. Bacterial cheating drives the population dynamics of cooperative antibiotic resistance plasmids. Molecular Systems Biology 9:683.
8. Pearl Mizrahi S, Goyal A, Gore J. 2023. Community interactions drive the evolution of antibiotic tolerance in bacteria. Proceedings of the National Academy of Sciences 120:e2209043119.
9. Bottery MJ, Matthews JL, Wood AJ, Johansen HK, Pitchford JW, Friman V-P. 2022. Inter-species interactions alter antibiotic efficacy in bacterial communities. 3. ISME J 16:812–821.
10. Medaney F, Dimitriu T, Ellis RJ, Raymond B. 2016. Live to cheat another day: bacterial dormancy facilitates the social exploitation of β-lactamases. 3. The ISME Journal 10:778–787.
11. Bottery MJ, Pitchford JW, Friman V-P. 2020. Ecology and evolution of antimicrobial resistance in bacterial communities. The ISME Journal 1–10.
12. Amanatidou E, Matthews AC, Kuhlicke U, Neu TR, McEvoy JP, Raymond B. 2019. Biofilms facilitate cheating and social exploitation of β-lactam resistance in Escherichia coli. 1. npj Biofilms Microbiomes 5:1–10.

13. Brännström Å, Johansson J, Von Festenberg N. 2013. The hitchhiker's guide to adaptive dynamics. 3. Games 4:304–328.
14. Vega NM, Gore J. 2014. Collective Antibiotic Resistance: Mechanisms and Implications. Curr Opin Microbiol 21:28–34.
15. Sorg RA, Lin L, van Doorn GS, Sorg M, Olson J, Nizet V, Veening JW. 2016. Collective Resistance in Microbial Communities by Intracellular Antibiotic Deactivation. PLoS Biology 14.
16. Frost I, Smith WPJ, Mitri S, Alvaro •, Millan S, Davit Y, James •, Osborne M, Pitt-Francis JM, Maclean • R Craig, Foster KR. 2018. Cooperation, competition and antibiotic resistance in bacterial colonies. The ISME Journal 12:1582–1593.
17. Geyrhofer L, Ruelens P, Farr AD, Pesce D, Visser JAGM de, Brenner N. 2022. Minimal Surviving Inoculum in Collective Antibiotic Resistance. mBio 14:e02456-22.
18. Alan Dugatkin Ã L, Perlin M, Scott Lucas J, Atlas R. 2005. Group-beneficial traits, frequency-dependent selection and genotypic diversity: an antibiotic resistance paradigm. Proc R Soc B 272:79–83.
19. Ruelens P, de Visser JAG. 2021. Choice of β-lactam resistance pathway depends critically on initial antibiotic concentration. Antimicrobial Agents and Chemotherapy.
20. Salverda MLM, De Visser JAGM, Barlow M. 2010. Natural evolution of TEM-1 β-lactamase: experimental reconstruction and clinical relevance. FEMS Microbiology Reviews.
21. Lautenbach E, Patel JB, Bilker WB, Edelstein PH, Fishman NO. 2001. Extended-Spectrum β-Lactamase-Producing Escherichia coli and Klebsiella pneumoniae: Risk Factors for Infection and Impact of Resistance on Outcomes. Clinical Infectious Diseases 32:1162–1171.
22. Ramphal R, Ambrose, PG. 2006. Extended-Spectrum β-Lactamases and Clinical Outcomes: Current Data. Clinical Infectious Diseases 42:S164–S172.
23. Hall BG. 2002. Predicting Evolution by In Vitro Evolution Requires Determining Evolutionary Pathways. Antimicrobial Agents and Chemotherapy 46:3035–3038.

24. Knies JL, Cai F, Weinreich DM. 2017. Enzyme Efficiency but Not Thermostability Drives Cefotaxime Resistance Evolution in TEM-1 β-Lactamase. Molecular Biology and Evolution 34:1040–1054.

25. Dugatkin LA, Perlin M, Lucas JS, Atlas R. 2005. Group-beneficial traits, frequency-dependent selection and genotypic diversity: an antibiotic resistance paradigm. Proc R Soc B 272:79–83.

26. Sharma A, Wood KB. 2021. Spatial segregation and cooperation in radially expanding microbial colonies under antibiotic stress. 10. ISME J 15:3019–3033.

27. Kim SW, Park SB, Im SP, Lee JS, Jung JW, Gong TW, Lazarte JMS, Kim J, Seo J-S, Kim J-H, Song J-W, Jung HS, Kim GJ, Lee YJ, Lim S-K, Jung TS. 2018. Outer membrane vesicles from β-lactam-resistant Escherichia coli enable the survival of β-lactam-susceptible E. coli in the presence of β-lactam antibiotics. 1. Sci Rep 8:5402.

28. King ES, Maltas J, Weaver DT, Barker-Clarke R, Pelesko J, Dolson E, Scott JG. 2022. Fitness seascapes are necessary for realistic modeling of the evolutionary response to drug therapy. bioRxiv https://doi.org/10.1101/2022.06.10.495696.

29. Blair JMA, Webber MA, Baylay AJ, Ogbolu DO, Piddock LJV. 2015. Molecular mechanisms of antibiotic resistance. 1. Nat Rev Microbiol 13:42–51.

30. Cartagena AJ, Taylor KL, Smith JT, Manson AL, Pierce VM, Earl AM, Bhattacharyya RP. 2023. The carbapenem inoculum effect provides insight into the molecular mechanisms underlying carbapenem resistance in Enterobacterales. bioRxiv https://doi.org/10.1101/2023.05.23.541813.

31. Estrela S, Brown SP. 2018. Community interactions and spatial structure shape selection on antibiotic resistant lineages. PLoS Comput Biol 14:e1006179.

32. Kogenaru M, Tans SJ. 2014. An improved Escherichia coli strain to host gene regulatory networks involving both the AraC and LacI inducible transcription factors. J Biol Eng 8:2.

33. Cronan JE. 2006. A family of arabinose-inducible Escherichia coli expression vectors having pBR322 copy control. Plasmid 55:152–157.

34. Schenk MF, Szendro IG, Krug J, Visser JAGM de. 2012. Quantifying the Adaptive Potential of an Antibiotic Resistance Enzyme. PLOS Genetics 8:e1002783.

35. Wiegand I, Hilpert K, Hancock REW. 2008. Agar and broth dilution methods to determine the minimal inhibitory concentration (MIC) of antimicrobial substances. Nature Protocols.

36. Balouiri M, Sadiki M, Ibnsouda SK. 2016. Methods for in vitro evaluating antimicrobial activity: A review. J Pharm Anal 6:71–79.